# RESEARCH PROJECT IN MECHATRONICS ENGINEERING

PART IV PROJECT FINAL REPORT

**LIMIT-TESTING OF THE HUMAN PERCEPTION OF BIOLOGICAL MOTION IN THE PERIPHERAL FIELD OF VIEW**

Joseph Byrne

Project Report ME037-2022

Co-worker: Alan Chen

Supervisor: Dr Luke Hallum

Department of Mechanical and Mechatronics Engineering
The University of Auckland

13 October 2022

**LIMIT-TESTING OF THE HUMAN PERCEPTION OF BIOLOGICAL MOTION INTO THE PERIPHERAL FIELD OF VIEW**

**Joseph Byrne**

## ABSTRACT

The human perception of biological motion (POBM) is an age-old evolutionary tool with enormous survival value. The contents of this report investigate the effect peripheral eccentricity has on the perceptibility of point-light walkers moving in different directions relative to an observer. Twelve subjects were trialed over four blocks each, yielding a total of 48 blocks worth of data. Results were averaged across this range, and psychometric curves were fitted to the data using the Weibull cumulative distribution function. POBM is shown to be deeply hindered by increased peripheral eccentricity, resulting in a general critical threshold margin of approximately +7 dots. The same is true in the viewpoint dependency paradigm, however, the frontal viewpoint emerged as the most consistently successful among its counterparts. A curious finding is one pertaining to the profile viewpoint. This was shown to be nearly as recognisable as the frontal viewpoint in the foveal field of vision, but its intelligibility became unscalably poor in the peripheral - suggesting a rapid decay in recognition (more so than from other viewpoints) for profile walkers. Previous literature has found there to be poor POBM in small ranges of peripheral eccentricity. We conclude that over great ranges of eccentricity, POBM is unsalvageable.

# Table of Contents

## List of Figures



## List of Tables

## Acknowledgements


| | |
|---|---|
| **Dr. Luke Hallum**<br>*Supervisor and Mentor* | We would like to thank Dr. Hallum for his guidance, advice and enduring patience. This project would not have been possible without his supervision and assistance. |
| **Alan Chen**<br>*Project Partner* | I would like to acknowledge and thank Alan Chen for his tenacity, and overwhelming positive attitude. Without his motivation and hunger for knowledge, this project would not have been completed to the degree it has been. |
| **Jerry Zhang, Carl Tang, Kevin Lee**<br>*Post-Graduate Mentors* | We would like to extend our gratitude to each of our post-graduate mentors. Thank you for your time, patience and guidance, without your ceaseless and helpful input, the project would not be what it is today. |
| **Luke Patterson, Bailey Sutton, Joseph Darge etc.**<br>*Experiment Subjects* | To our subjects, thank you for your patience and time. The data provided by our subjects made our analysis and results possible. |
| **Emmanuelle Romano**<br>*Lab Technician* | Without the training you graciously provided, our understanding of both Motion Capture and BCI would have been sub-par for the completion of this project - thank you. |

## Glossary of Terms

| | |
|---|---|
| *Atypical Viewpoint* | Either intermediary (30° or 60° azimuth) viewpoints |
| *Azimuth* | The horizontal (non-elevational) direction from an observer to an object or stimuli |
| *Fovea* | The clearest region in the center of the human field of view |
| *Percept* | The object of an observer's perceptual focus |
| *Primary Joint* | One of a set of joints used primarily in walking or other human motion (include ankles, shoulders, knees, elbows etc.) |
| *Typical Viewpoint* | Either frontal (0° azimuth) or profile (90° azimuth) viewpoints |
| *Visual Noise* or *Degradation* | Addition (or removal) of stimuli which serves to abstract the original, untouched stimuli |

## Abbreviations

| | |
|---|---|
| *4AFC* | Four Alternative Forced Choice |
| *CDF* | Cumulative Distribution Function |
| *EMI* | Electromagnetic Interference |
| *FOV* | Field of View |
| *MCC* | Matthew's Correlation Coefficient |
| *MCT* | Mean Critical Threshold |
| *MoCap* | Motion Capture |
| *PLW* | Point-Light Walker |
| *POBM* | Perception of Biological Motion |
| *WCDF* | Weibull Cumulative Distribution Function |

# 1. Introduction

## 1.1 Overview

Visual perception is a miraculous tool which enables even the most infantile of its aspirants to gather and compress known truths about their surroundings. Once visually informed, we may navigate what may have otherwise been considered a treacherous domain. Our visual perception is comprised of near-enumerable, evolutionary mechanisms each with distinct survival value - one of which is our capability to perceive biological motion. Aptly dubbed "a perceptual life detector" [1], this skill pertains to one's ability to discern animate objects from an inanimate environment - sometimes in a matter of milliseconds [2]. This phenomenon has been observed in infants, the neurologically disaffected, and even animals, making it - to our knowledge - a universal capability [2–5]. The first to devise a strategy to accurately brass-tack POBM experimentally was Dr. Gunnar Johansson (et al.) [6]. It was proposed that a mere dozen dots representing the primary joints on a human physiology would provide a rich impression of the human gait (figure 1). This is now known as a point-light walker.

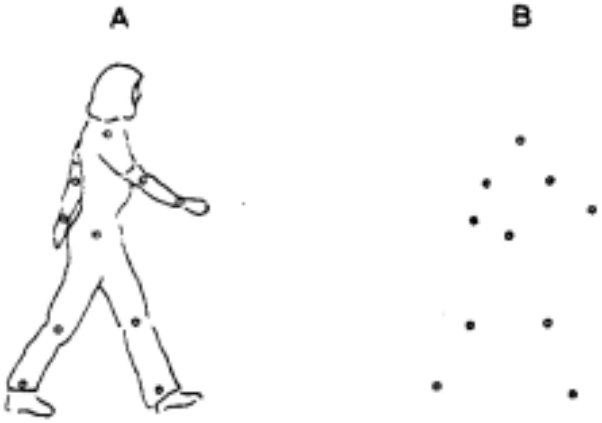


**Figure 1** Walking subject (A) and their PLW representation (B). Retrieved from [6].

One's visual field of view can be divided into two principal categories - foveal and peripheral (or so-called extrafoveal). Given the application of foveal vision, the vast majority of literature in this field investigates the limits of POBM in the foveal. Curiously, since Johansson's developments, very little investigation has been carried out regarding POBM's application in the human peripheral, and whether the peripheral - with its inherent perceptual transformations - has tangible effect on POBM.

## 1.2 Objectives

Through the completion of this investigation, we aim to illustrate and quantify:

- The adaptivity of *a priori* perceptive sensory capabilities
- The resourcefulness of human vision and processing
- The effects of *peripheral vision* on the POBM
- The effects of *typical and atypical viewpoints* on the POBM
- The effects of *visual degradation* on POBM

### 1.3 Our Hypotheses

We have developed **three** primary hypotheses which we wish to test in tandem within this experiment. We theorise that human POBM will:

1. degrade in the periphery,
2. degrade with increased visual degradation, and
3. be impaired in atypical viewpoints

### 1.4 Project Scope

The contents of this report will endeavour to investigate and consequently quantify the effects of peripheral vision on POBM. It will also research the effects of visual degradation and viewpoint type - seeking to test the aforementioned hypotheses. The gait presented to test subjects will be illustrated in a looped video format of a point-light walker (PLW) and will indicate to the subject the motion of a variety of the major joints in human physiology. To degrade the visual stimuli, we will utilise a variety of techniques such as noise, point lifetime, and inversion. This will enable us to determine the bounds of the human vision's resourcefulness.

# 2. Literature Review

## 2.1 Current State of the Field

### *2.1.1 Historical and Present Direction*

As aforementioned, [6] was responsible for the **first steps** in this field of research. Johansson et al. determined that the human ambulation could be perceived just as vividly with the discretisation of the human body into several points of light. This breakthrough gave rise to a slew of others made in subcategories of the newly developed field and his developments had far-reaching implications. For example - Vallortigara et al. demonstrated that newly hatched chicks who had no prior experience in visual stimuli, exhibited biological motion preferences [3]. Neurodegenerative subjects have also been a point of study within the field [7].

Recently, progressing technology has provided the necessary platform for the development of a modelling technique capable of correctly discerning the direction of human motion. POBM has been cited as a potential modelling technique from which autonomous vehicles (AVs) may discern the direction in which a pedestrian is traveling relative to the AV's own motion [8]. This means that further defining this field could assist in a variety of applied computer vision advancements too.

### *2.1.2 Readily Available Data*

Given the relative novelty of the field's research, it stands to reason that the availability of relevant datasets is equally limited in both their abundance and relevance. At present, the main body of datasets is available on an open-source platform called PhysioNet. Made available are some arbitrary datasets pertaining to the observed ambulation of specific groups of people, including; those with Parkinson's disease (PD), neurodegenerative diseases, and those who are aging and/or diseased [9]. Based on this assessment of the available data and the relative novelty of the field, any data-based contribution to the field would certainly be of value.

## 2.2 Peripheral Vision

Foveal vision covers approximately 1.7° of the central visual field. The region outside of the fovea comprises approximately 99.9% of the visual field - termed the peripheral region [10]. Peripheral vision is known broadly as the region of vision in which a given percept may be distorted. Distortion can involve diminishment, enlargement or more complex distortion of an image (such as the proverbial *blur*, see figure 2). That said, the peripheral is not entirely impoverished - as one may misconceive it to be. Instead, humans have up to 60° of operable FOV in the temporal azimuth direction (away from the nose, toward the ear) [10].


**Figure 2** Original image (a), distortion applied to mimic human vision (b), distortion accentuated further for ease of observation (c). Retrieved from [10].

Peripheral vision has been shown to have an effect on POBM, but this has yet to be framed with the sort of visual degradation and viewpoint dependency that this report handles. For example, [11] - one of the only other studies of this nature - investigated the dependency of POBM on peripheral eccentricity. However, they made use of minutely different viewpoint angles, a small eccentricity range, and *superimposition* visual noise techniques (discussed in subsequent sections). They concluded that peripheral eccentricity had unscalably negative impacts on POBM. We wish to investigate the effects of peripheral eccentricity on POBM over a far greater range.

### 2.3 Point-Light Walker Configurations

PLWs are collections of discrete points that are used to represent the motion of the joins and key appendages of the human (or other species') body (figure 1). This is done via motion capture, using a MoCap laboratory fitted with an array of cameras that are highly sensitive to reflected light. The capture subject is laden with reflective nodes that are accentuated by the motion capture cameras to produce a PLW in three dimensions. Three dimensional timeseries data are necessary to render a PLW to a quality accurate enough for experimentation (especially for viewpoint exploitation).

PLW configurations provide a pathway to achieving different levels of abstraction and ambiguity regarding the walker's motion. Wood et al. investigated the implications of varying PLW configurations on the obscurity of their respective walker's direction of motion. They made clear conclusions that more nodes (reflective strips on road workers) resulted in greater conspicuity [12]. There is, however, a relative plateau of subject performance at which the PLW becomes saturated and thusly the subject can correctly determine the direction of motion with consistency. This *plateau number* depends on the experiment and the visual degradation at play. Some investigations have sought to generate synthetic PLWs with some degree of success [13]. PLWs could also have great application to the aforementioned technologies (figure 3).

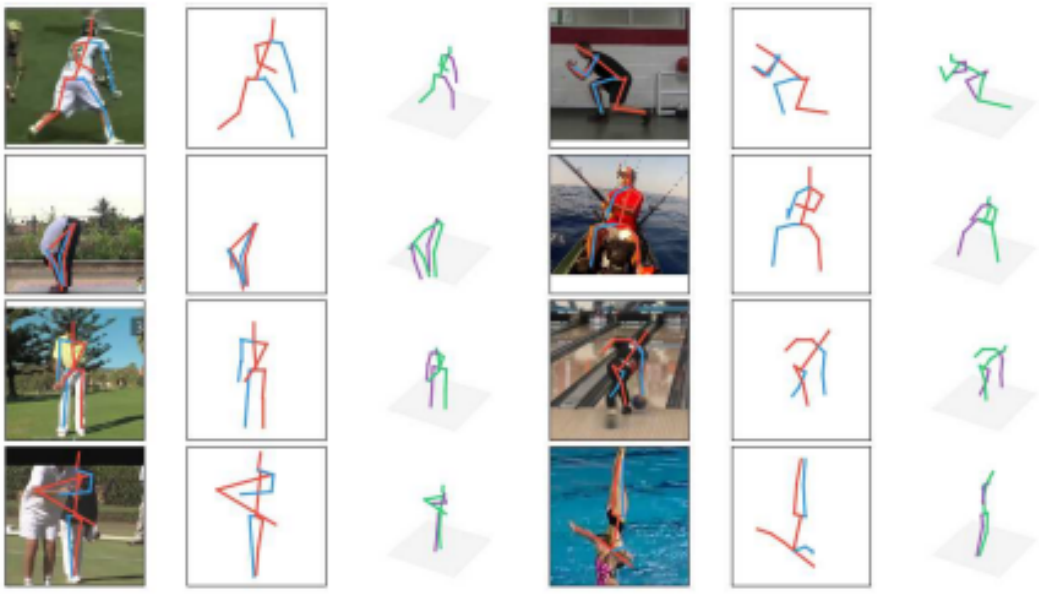

**Figure 3** Extrapolation of PLWs into line geometries representing human pose estimations. Applicable to many different human poses - not just ambulation. Retrieved from [14].

### 2.4 Viewpoint Types

One can observe from personal experience that most objects are difficult to recognise when inverted (i.e. when we perceive that object from a viewpoint that is atypical relative to its common orientation). Facial recognition has been shown to be disproportionately impaired by inversion, an occurrence known as "the inversion effect" [15]. Reed et al. posited that although there are no registered inversion effects in non-face objects (e.g., flowers, houses), there could be an inversion effect in body recognition, too. They presented the first evidence that this may be the case [16], and this naturally highlights atypical viewpoints as a worthwhile point of investigation.

Present-day software has the capability to represent a PLW in a three-dimensional (3D) plane, and thus the number of viewpoints is infinite. The procession of this report will primarily deal with four viewpoints (table 2) - two typical and two atypical.

It has been concluded that atypical viewpoints (PLW directions), for the most part, are harder to decipher than their typical counterparts [17]. This incoherence can be attributed to the human reliance on the geometric information provided by the finite group of standardised connectivity patterns. In other words, humans require connectivity information to inform their POBM. In atypical viewpoints, the connectivity patterns between primary nodes are not as apparent as in typical viewpoints, thus degrading a given subject's POBM for atypical viewpoints.

| NAME | CLASS | ANGLE (DEG.) |
|---|---|---|
| FRONTAL (F) | Typical | 0 |
| FRONTAL AZIMUTH (FA) | Atypical | 30 |
| PROFILE AZIMUTH (PA) | Typical | 60 |
| PROFILE (P) | Atypical | 90 |

**Table 2** Viewpoints addressed in this project and their classifications

### 2.5 Visual Stimuli Degradation

It is suitable to visually degrade stimuli in experiments such as ours as we are seeking an understanding of subject performance. To quantify this, we require a criterion for comparison - such as a performance threshold, achieved only by tuning the difficulty of the experiment. Moreover, the degradation further serves as a mimicry of real-world occlusion of key joints in the human physiology as they walk. There are several methods via which a number of independent investigations have visually degraded the visual stimuli produced by PLWs (figure 4).

In [18], visual noise was introduced (which involved the superimposition of additional dots onto the original PLW), and subjects were directed to identify the direction of biologic motion at different levels of noise. Moreover, Beintema et al. investigated both limited-lifetime stimuli and PLW configurations as methods to visually degrade the displays. They found that whilst PLW configuration (i.e., the reduction of points) had a significant effect on perception, there was no observable effect resulting from limiting the point lifetimes [19]. Most notably, Beintema et al. did not randomly allocate lifetimes to points, nor did they test the two in tandem - which could be of use.

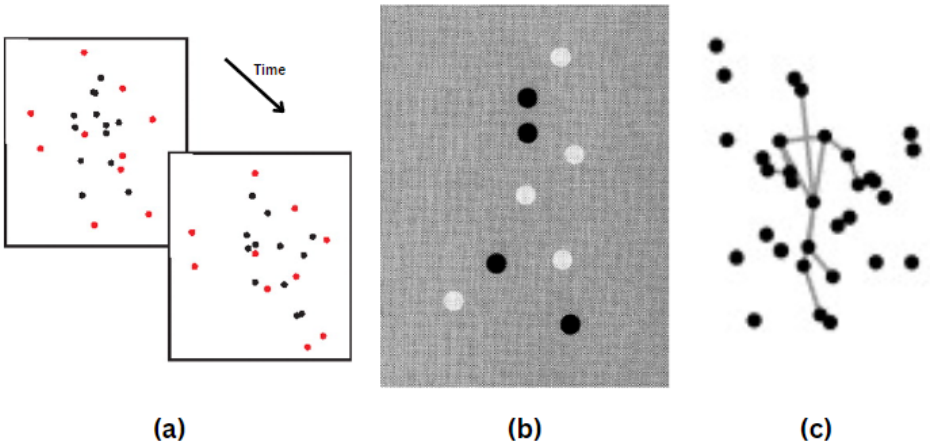


**Figure 4** Different methods of visual degradation seen in other studies in the field. Point "morphing" (a) seen in [20], contrast manipulation (b) seen in [21], and superimposition (c) seen in [11].

## 2.6 Gap Identification

There has been comprehensive study into the foveal application of POBM, yet as stated above, peripheral vision makes up approximately 99 per cent of the human FOV. Curiously, investigation of the peripheral's implications on POBM is yet to truly take form. Furthermore, alternative viewpoint and visual degradation testing has also yet to be applied in the peripheral-vision-POBM paradigm. There is only one source of literature truly comparable to our line of research, and this source uses different viewpoint experimentation and degradation techniques. Given the infancy of the topic within the field, the scarcity of study on this topic, and the conclusions the relevant literature has made, we can be sure that our experimental direction will be novel and valuable in the field.

# 3. MoCap Data

## 3.1 Overview

To produce and render the stimuli required for accurate testing, 360° time-series data was necessary. We needed to be able to process the captured data such that we could freely rotate or transform the stimuli (in post-processing) to be fit for the experiment. Furthermore, we needed to render this data as a point-light walker (not a contour or geometric skeletal model), and as such required the removal of any human features from our ambulation volunteer.

## 3.2 Data Capture

To capture the required data, we used the MoCap laboratory - courtesy of the University of Auckland. This laboratory was furnished with an array of 14 100Hz LiDAR cameras spanning a 360° range around the perimeter of the capture room. To remove any unwanted geometry or features from the capture, we ran the capture in high-contrast mode. Our volunteer was a 5-foot-8-inch, 22-year-old male. We fitted him with a total of 28 retroreflective nodes (encompassing each of his primary joints) - which reflect light to an extremely high degree in three dimensions (figure 5). Given the nature of the capture room, any nodes occluded to one camera within the array, were certainly visible to another in the array (granted the volunteer was in the geometric center of the capture room).


**Figure 5** Volunteer fitted with retroreflective nodes from front (a) and rear (b).

We had the volunteer walk on a treadmill at a nominal speed of $1.5\text{ms}^{-1}$ over a duration of 60 seconds. Having our volunteer walk on a treadmill simplified the data processing significantly, as we did not need to remove the volunteer's translational motion. The high-contrast mode in conjunction with the retro-reflective nodes enabled us to capture and process the volunteer's ambulation over the test period. The data was processed using software called ViconNexus™, which generated a time-series data set comprising the Cartesian coordinates of each of the nodes throughout the duration of capture.

### 3.3 Data Processing

With the Cartesian time-series data exported from ViconNexus™, we were able to extract the trajectories for each of the 28 nodes. We could subsequently parse the trajectories via a transformation matrix, $\boldsymbol{M_T}$, with angle input to render a walker at any viewing angle we desired. Because the the trajectories are projected onto a 2D plane in ViconNexus™ and MATLAB® a simplified-three-dimensional transformation is required (transforming about the Z-axis - the Z-axis being the vertical axis; ground-upwards) (figure 6, equation 1).

$$\hat{x}' = \boldsymbol{M_T}\hat{x} \rightarrow \begin{bmatrix} x' \\ y' \\ z' \end{bmatrix} = \begin{bmatrix} cos(\theta) & sin(\theta) & 0 \\ -sin(\theta) & cos(\theta) & 0 \\ 0 & 0 & 1 \end{bmatrix} \begin{bmatrix} x \\ y \\ z \end{bmatrix} \tag{1}$$

To process the data and finally render it into a 2D PLW, we a used toolbox within MATLAB® called `PsychToolBox`. `PsychToolBox` enables its users to render visual and audio stimuli for sensory testing purposes. It is equipped with helpful functionality for accurately presenting and manipulating MoCap data. `PsychToolBox` also enabled us to manipulate dot size, walker speed (using frame rate), and walker size - all of which we based upon Troje et. al, a prolific scholar and publisher in the field [22, 23]. It is worth noting that the orthogonal nature of the stimuli produced presents an issue of perspective in that the dot sizes (and spaces between dots) are not scaled based on distance from the observer. However, since the walker is 2D and Johansson et al. made no remark regarding this matter (nor did any other sources we found useful in the development of the walker), we decided to omit this from our considerations [6].

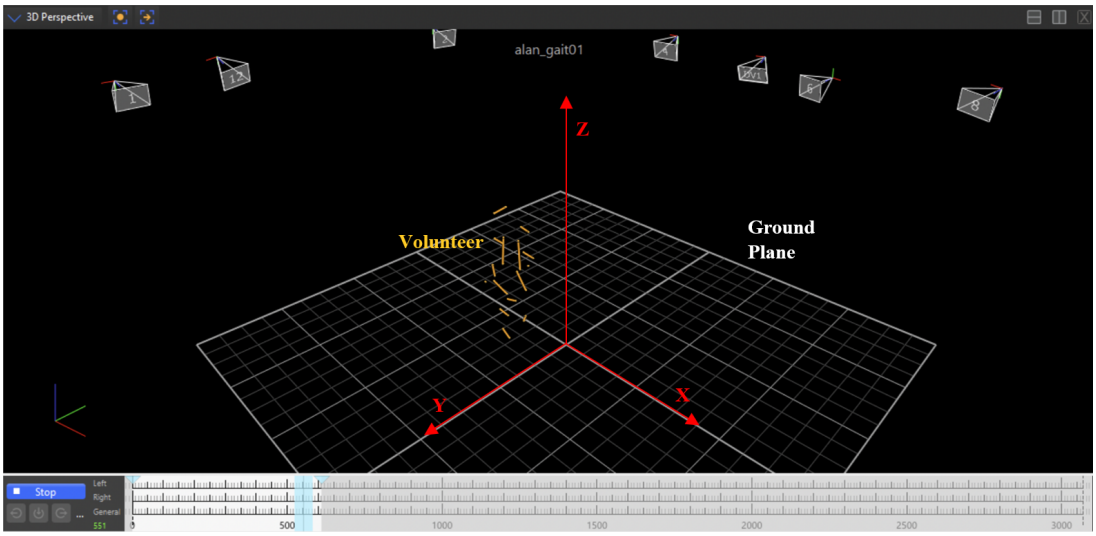


**Figure 6** ViconNexus™ data capture environment, note the floor plane and superimposed axes.

# 4. Experimental Methods and Decisions

## 4.1 Overview

We were able to enlist a total of 12 participants for trial in our experiments, each of them affiliated with the University of Auckland. A key consideration before amassing this group was to first devise an experiment that would not be overly tedious to complete, but also captured data relevant to our objectives. As such, the following section will discuss our trialing technique, and the decisions made concerning experimental design to ensure all collected responses were relevant. It is important to note that we first gathered pilot data in order to validate the experimental design, before proceeding to real trials. These preliminary trials informed us of a handful of useful improvements which will be discussed subsequently.

## 4.2 Independent Variables

### *4.2.1 Visual Degradation*

As mentioned prior, visual degradation (and noise) are used to reduce subject success rates to a critical level or even the guess rate. This can be tuned to produce a success-rate-degradation relationship. There are several methods by which an assessor may implement visual degradation, we elected to proceed with a hybrid implementation of both dot lifetime, and dot removal. These two have not been tested extensively in the literature in the paradigm of the peripheral. They also represent an opportunity to easily reduce the acuity of the stimuli, which will guarantee the discovery of a critical dot threshold with reference to the subject success rate. We chose to reduce the lifetime of each dot to 200ms and rendered the stimuli visible for only 1s. This meant that the stimuli would cycle through 5 uniquely random sets of dots (the number of which depended on the level of degradation) representing the same walker at its given viewpoint angle, before clearing the screen.

### *4.2.2 Viewpoints*

Because the only other peripheral literature in the frame of POBM tested with very minute changes in viewpoint angle, we saw fit to test with larger increments, to ascertain the peripheral's effects on a greater range. This does mean we sacrifice specificity, however, it will inform more so the differences between each angle (if there are any to be found). As such, we elected to proceed with angles indicated in table 2 and figure 7.

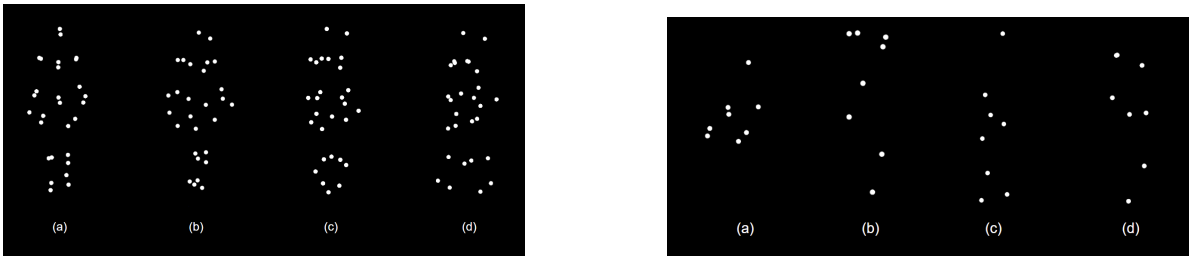


**Figure 7** Viewpoints - F (a), FA (b), PA (c), P (d), displayed to the subjects using MATLAB®, produced with `PsychToolBox`. Note the left image is the untouched PLW, and the right image is visually degraded.

It is important to note that the viewpoints will be the medium for testing subject success rate (i.e., the experiment will be a four-choice forced alternative). As such, it makes sense to provide choices that are sufficiently different in their untouched form, so as to reduce the amount of guessing and thus false positives.

### *4.2.3 Peripheral Eccentricity*

Following with the theme above of pursuing a larger range than in [11], we elected to push the limits of the perceivable peripheral vision, as in [10], to 0° - 40°. This increment makes it easy to discern any clear effects due to peripheral eccentricity. Moreover, it sets our investigation apart from others and adds distinct value to the data we gather. Finally, because the maximum eccentricity is at the bounds of the range of acuity, we may find results unique to the topic as this range has not been tested in the POBM field.

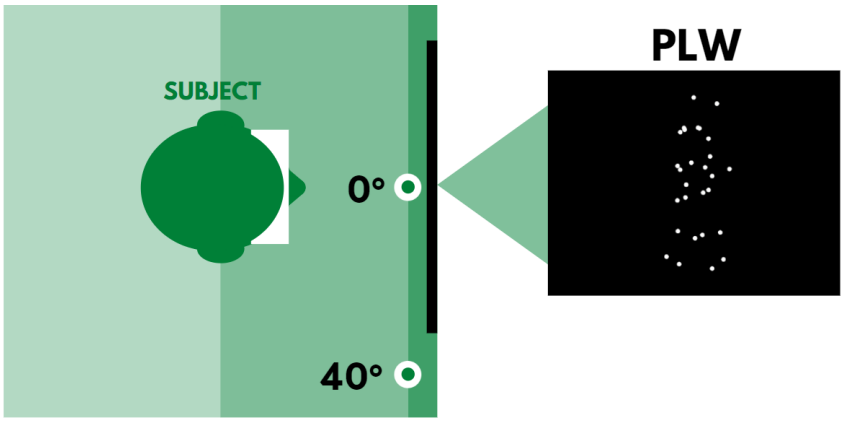


**Figure 8** Subject apparatus used to control subject visual eccentricity. Note the 0° and 40° markers used to direct the subject toward to correct eccentric angle from trial to trial. The subject was directed by indicating the trial's respective eccentricity before it began - the program would then wait for user input before initiating the trial (figure 11).

## 4.3 Experimental Design

To ensure that the data was entirely unbiased, we randomized as much of the experiment as possible. We conducted a complete block of trials, randomly iterating through each set of independent variables as we did so (figure 9, left). We elected to proceed with a 4CFA experimental design in which the subject was prompted to select one of four viewpoint angle submissions (figure 11). Each subject ran through four blocks of the same set of trials, however, each block's trials were randomised on a normal distribution as per MATLAB®'s randomisation function. The subject's successes were logged into a `.mat` file including their success matrices (figure 9, right), their name, and the number of trials they completed - for all subjects this number was four.

| VARIABLE | INCREMENTS |
|---|---|
| ECCENTRICITY | 0°, 40° |
| VIEWPOINT ANGLE | 0°, 30°, 60°, 90° |
| NUMBER OF DOTS | 2, 4, 8, 12, 16, 20, 24 |

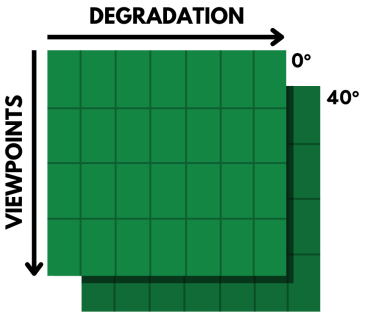


**Figure 9** Selected increments (pursuant to what has been discussed in prior sections) for the experiment (left), and 3D storage matrix for subject data (right).

In hindsight, an improvement that could have been made here is the storage of answer data as opposed to success singularly. This way we could have subsequently plotted confusion matrices and determined the difference in POBM for differing viewpoints using specificity, sensitivity, and accuracy (using the likes of MCC [24]). That said, the data gathered is enough to determine the relationship between peripheral vision and POBM.

### 4.4 Experimental Conditions

Given the perceptual nature of our investigation, it made sense to deprive all other senses to the point at which visual perception became paramount. As such, we conducted our experiment in the brain-computer-interface (BCI) lab. The BCI lab is fitted with acoustic soundproofing, as well as complete blackout conditions, and even a room-wide EMI shield. Because of these furnishings, it was the perfect environment for our experiments. To remove external visual noise we blacked out the room - except for the screen displaying our stimuli, and reserved the room for our exclusive use.

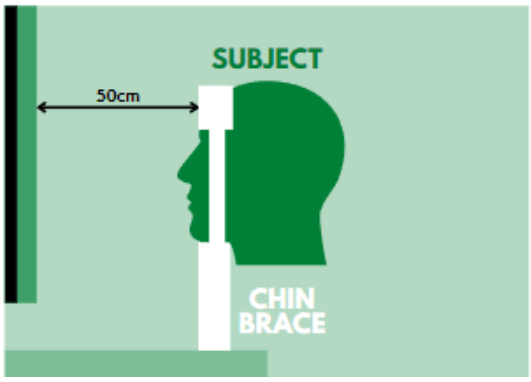


**Figure 10** Subject apparatus used to control eccentricity and cornea-stimuli distance. 50cm distance used for similarity with [11], which used 57cm.

Furthermore, we fitted a chin and head brace on a swivel to control the distance from our subject's cornea, to the stimuli. This brace also enabled the subject to turn their head slightly, should the block of trials become straining at any point. We were extremely conscious of the strain the experiment could place upon our subjects, and thus we were sure to explain and disclaim the experiment profusely before the subject undertook any trials. Moreover, the stimuli themselves could be quite jarring initially: we discovered in our pilot data that subjects performed worse in the initial 10 trials than in the ensuing trials. Because of this, we implemented a 'practice run' block of 10 trials to help our subjects acclimatise to the stimuli and test conditions.

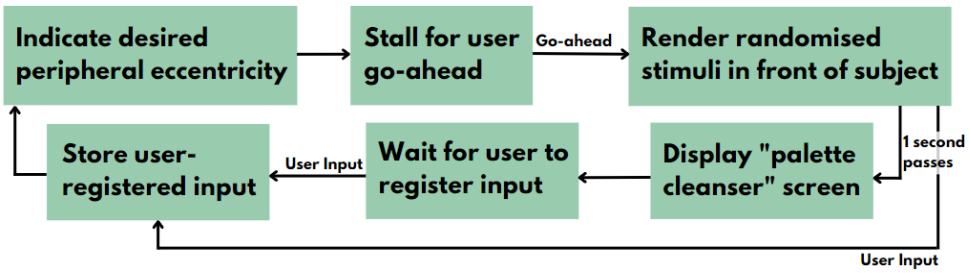


**Figure 11** Block diagram indicating the experimental design and procession of our trials. The palette cleansing screen in our case was a bright red screen (as visually different from the rendered stimuli as possible). It is worth noting that the palette cleansing screen serves to proverbially "clear the memory" of our subject prior to the next trial.

# 5. Data Analysis

## 5.1 Overview

To determine whether the data gathered could yield reliable conclusions, we needed to perform rigorous statistical testing. Although the sample space is a fair size relative to other investigations within the field, it is not enough to simply generalise the mean performance of our subjects and call it reliable. Further investigation as to the solidarity, applicability, and robustness of our conclusions is required. To do so, we first analysed the raw data - this gave us a general idea of what we should see in the statistical analysis. We then fitted psychometric (technically speaking, sigmoidal) curves and conducted an analysis of the critical threshold, before bootstrapping the data and conducting this analysis over multiple iterations. To expand, analysis via the critical threshold is commonly used to define the "tipping point" of some psychometric mechanism [11, 12]. The critical threshold is defined as the number of nodes at which the subject success rate falls below 62.5% (halfway between guessing and 100% correct). We also analysed viewpoint dependency through the same methods described above (see appendix B.1).

## 5.2 The Raw Data

The raw data plotted is simply the mean success rate across 12 subjects at four blocks each. This equates to a total of 48 blocks or 48 trials per random combination of independent variables. As such, each point plotted is the average success rate for all subjects across 48 trials.

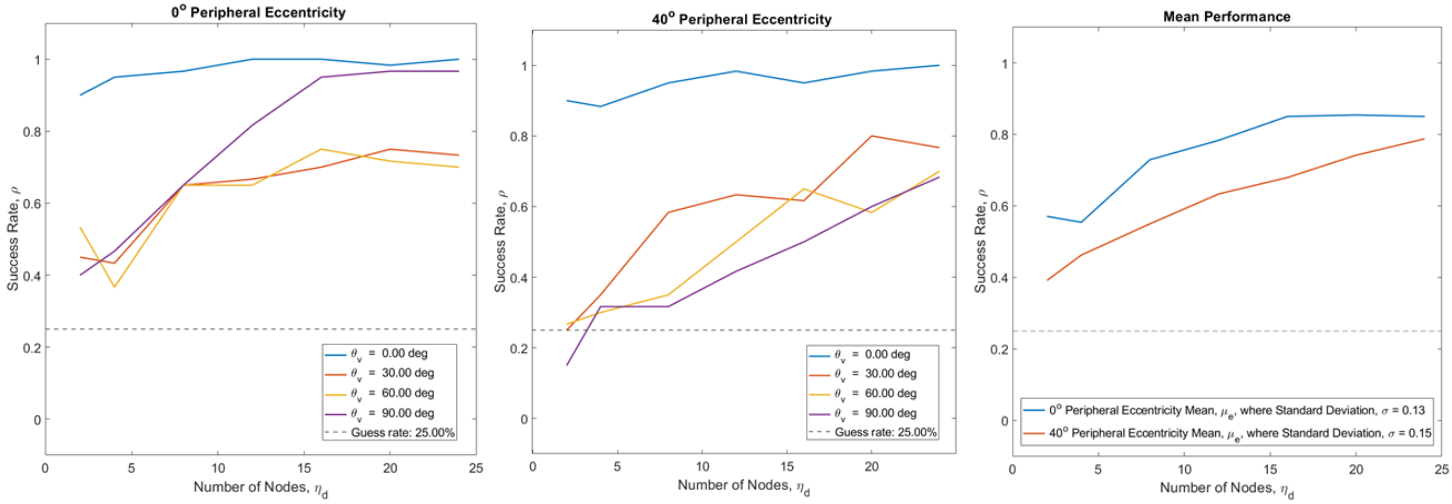


**Figure 12** Raw data collected from 12 subjects at four blocks each. See 0° (left) and 40° (middle) viewpoint performances as well as the overall mean subject performances for peripheral eccentricity (right).

There is a clear numerical difference in the two averaged datasets. However, we need to conduct a more rigorous statistical analysis to confirm what we see in the plot above. The same can be said for the viewpoint performances in both the peripheral and foveal. Though, it seems subjects perform better in both typical viewpoints than in their atypical counterparts. As such, what we anticipate from our further analysis is something along the lines of equations 2 & 3.

$$T_{C,0} < T_{C,40} \tag{2}$$

$$T_{C,F} < T_{C,P} \lesssim T_{C,FA} \approx T_{C,PA} \tag{3}$$

*Where $T_{C,I}$ is the critical threshold for the I° eccentricity or I-type veiwpoint.*
***N.B**: See table 2 for the relevant viewpoint abbreviations.*

## 5.3 Psychometric Analysis

### *5.3.1 Fitting a Psychometric Curve*

To further analyse the data, we sought to fit a psychometric curve to the data produced from both sets of mean performance data, as well as to the viewpoint data sets. A psychometric curve is a sigmoidal curve of best fit fitted to the provided data and used to derive interpolations and extrapolations of said data. One may select from a variety of cumulative distribution functions from which to derive a fitted sigmoid - initially we elected to use a Gaussian CDF. We found this function to be too rigid and unfavourable for our purposes, thus we ultimately used the "Weibull" sigmoid [25]. The Weibull sigmoid (it is worth noting that this WCDF sigmoid is derived from the probability density function of a random Weibull variable described in equation 4) affords its user more control - for example; forcing the curve through a given value (i.e. the guess rate) was useful for deriving a more accurate predictor.

$$P_{weibull} = \begin{cases} 0 & -\infty < x \leq \infty \\ 1 - e^{-x^{\beta}} & 0 < x < \infty, \beta > 0 \end{cases} \tag{4}$$

To plot the WCDF sigmoid on the raw data, we ran through 1000 iterations in which we attempted to reduce the sum of the squared error to a minimum. Once the mathematical cost of the fitted function was at a minimum or the iterations had been completed, we plotted the curve over the points along with their confidence intervals (figure 14).

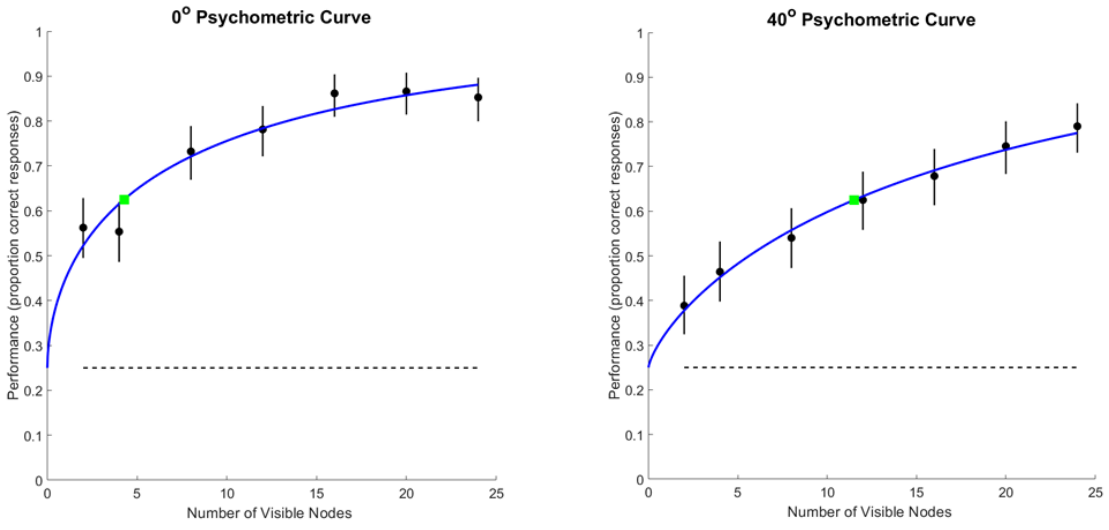


**Figure 13** Weibull psychometric curves fitted to the raw data for both zero (left) and forty (right) degree peripheral eccentricity. Shown in green are the critical thresholds (4.2763 and 11.5075 dots respectively). Notice our custom Weibull necessitates that the fitted curve passes through the guess rate at zero visible dots (25%), and looks to asymptote very close to 100% success rate.

Immediately, one might observe the clear difference in critical thresholds - this is as expected and certainly encouraging. To proceed we will fit many psychometric curves and determine whether our data is reliably accurate based on its re-sampled critical thresholds.

### *5.3.2 Bootstrapping the Data*

To bootstrap the data, we needed to randomly re-sample it a great number of times, fit new psychometric curves each time, and subsequently record the determine critical threshold. This enables us to stress test the data in a repetitive and iterative manner - re-sampling many times reduces the likelihood of our data being unreliable and inconsistent. We could then plot a histogram using the stored critical thresholds and, if the data is reliably consistent about a given mean value, observe a fairly normal distribution. Furthermore, we can determine whether the difference in the two datasets is statistically significant by observing no overlap in the spread of the two.

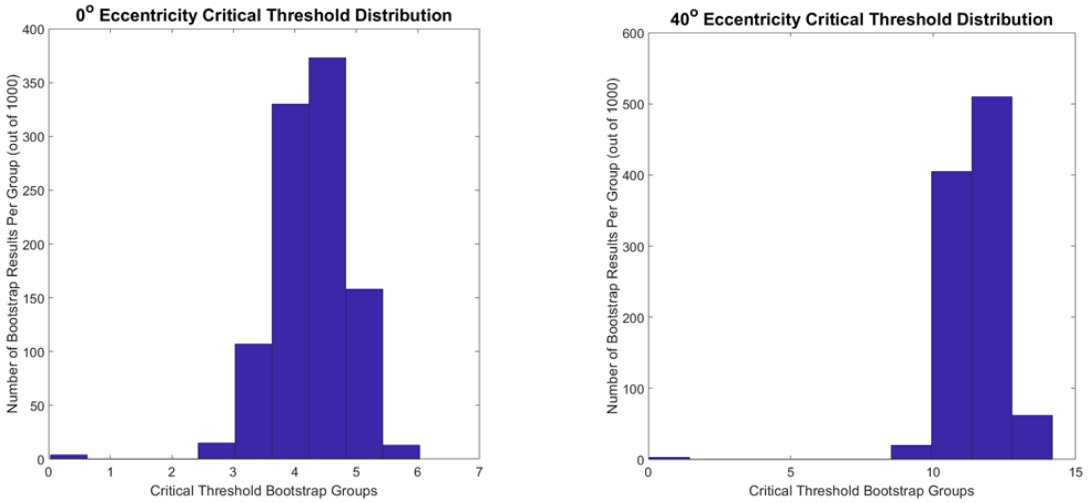


**Figure 14** Histograms representing the distributions of the critical thresholds, for all 1000 bootstrapped datasets, across both zero (left) and forty (right) degree eccentricities. The zero degrees distribution is normal with a mean value of 4.2749 dots and a forty-degree value of 11.5191 dots.

These plots indicate both dependable and statistically significantly separable data (after 1000 cycles of randomised, overlapped re-sampling). This can be concluded due to the absence of overlap in the two data sets (discarding the seemingly outlying case at 0 dots in both sets), in tandem with their normal distribution about a clear mean.

## 5.4 Viewpoint Dependency in the Periphery

To investigate the effect the peripheral may have on viewpoint dependency, we carried out an identical analysis (as above) for each viewpoint performance in each peripheral eccentricity. In the same way, we compare each foveal critical threshold to its peripheral counterpart to ascertain any quantitative difference in performance.

We observed a clear discrepancy (as expected) between the eccentricities. However, this analysis unveiled some peculiar interactions. Firstly, noting the frontal results, we observe an ***extremely*** low mean critical threshold. This is sensible given the nature of our collected data - we observe a high success rate for both peripheral variants of the frontal viewpoint. Secondly, the atypical viewpoint performances are extremely close to one another, and are degraded in the peripheral. The foveal performance for atypical viewpoints is also marginally worse than for typical viewpoints. The intriguing result is that which belongs to the profile viewpoint. Worse performance in the foveal than its frontal counterpart

is sensible. However, the drastic leap to such a great threshold in the peripheral is confounding. This effect has yet to be observed in the literature and may be a point of further investigation.

It is worth noting that though the data indicates some interesting conclusions, to reliably speak on the viewpoint interactions with POBM we need to carry out a sensitivity and specificity analysis. This is because the bloated frontal results or the poor peripheral profile results could simply be artifacts of the subject guessing - a confusion matrix would illuminate precisely when and what our subjects are guessing.

| | | ECCENTRICITY | |
|---|---|---|---|
| | | 0° | 40° |
| VIEWPOINT | F | 0.3118 | 0.1451 |
| | FA | 9.8595 | 12.9807 |
| | PA | 9.7043 | 14.4509 |
| | P | 6.8502 | 16.9332 |

**Table 3** MCT results of bootstrapped viewpoint data for each peripheral eccentricity. See table 2 for viewpoint clarification.

### 5.5 Statistical Conclusions

We observed firstly that there is a peripheral effect in the raw data on a superficial level. This informed us of what to consider in our statistical analysis. Secondly, we noted a clear difference in the critical thresholds determined by the psychometric curves produced by our raw data. This encouraged further investigation into the extrapolating and interpolating reliability of our further data and hinted at encouraging results. Finally, bootstrapping the data granted us a clear depiction of the difference in the peripheral eccentricities. We can conclude that there is a statistically significant difference between the MCTs for each eccentricity. Thus, we have ultimately observed a reduction in the human's POBM with increased peripheral eccentricity.

Regarding viewpoint dependency's interaction with peripheral vision - the observed effects are equally clear, but to be taken lightly pending further investigation. Bootstrapping the data presented a relation between viewpoint category and critical threshold. The frontal viewpoint is the easiest to perceive categorically, each atypical viewpoint (though more difficult to perceive than the profile in the foveal) is easier to perceive than the profile in the peripheral. This indicates some form of immediate decay in the POBM of the profile viewpoint and warrants further investigation. We would like to remind the reader that these observation are *strictly* reason for further study, and are not necessarily statistically conclusive. That said, each viewpoint case exhibits sensitivity to the distortion of peripheral vision - which is as expected given our mean data conclusions.

For the most part, predictive equations 2 & 3 have been validated. From table 3, we recognise a deeper level of specification is needed for 3. The relative viewpoint equation now becomes a pair (equations 5 & 6):

$$T_{C,F,0} << T_{C,P,0} < T_{C,FA,0} \approx T_{C,PA,0} \tag{5}$$

$$T_{C,F,40} << T_{C,FA,40} \approx T_{C,PA,40} \approx T_{C,P,40} \tag{6}$$

## 6. Discussion

Though our results seem relatively conclusive and have been statistically proven as reliable, it is worth discussing the caveats of this study, and where its accuracy and breadth may be improved. Furthermore, statistical results - though solid - may be less intuitive to the lay reader. As such, we would like to qualitatively analyse our results, and offer reasoning for the observed effects.

One potential misgiving of the investigation is its generalisation of all subjects - of course, some subjects performed far better (and far worse) than other subjects. The raw data - from which we extract all statistical conclusions - represents the mean subject performance across 12 subjects. Hence, though the data represents a fairly sizable sample space relative to other studies in the field, we cannot take its statistical conclusions as *concrete*. It is worth considering gathering a higher volume of data in future exploits. This is not to say that the data gathered is futile, instead simply that the conclusions reached are goalposts for further investigation. A second such pitfall could be the 4AFC structure of our experiment, wherein we may have somewhat over-saturated the decision plane for subjects. This may have led to subconscious guessing biases which could have resulted in falsely high (or low) readings for given viewpoints. For example, a subject may input a 0° response for all *guesses* - as opposed to randomly selecting one of four choices as assumed by the experiment. This would result in bloated readings for the 0° viewpoint angle and could falsely suggest a human sensitivity toward frontal walkers. It is worth noting that this may be the reasoning behind the rather poor performance in the profile viewpoint as compared to other atypical viewpoints in the peripheral. Despite this, these false readings should not influence the peripheral mean data or the peripheral conclusions made above.

Proceeding with the conclusions derived from the data - it is clear there is a distinction between human POBM in foveal and peripheral vision, but *what does this mean*? The critical threshold describes the number of dots at which the mean subject performance falls below the critical performance (i.e. 62.5%). If the number of dots described by the critical threshold is fewer for a given eccentricity, then we can conclude that human POBM is generally better at this eccentricity. Thus, given that the mean critical numbers of dots for 0° and 40° are 4.2749 and 11.5191 respectively, we can conclude that the human POBM in the foveal vision is better by a margin of approximately -7.2 dots. Though this is consistent with the conclusions found in [11], it is still a curious finding. Given the survival value of POBM, one would expect its application to be far-reaching across the span of the human FOV. However, we and [11] have both found that this is not the case. What's more is our degradation techniques and eccentricities were more aggressive than in [11], yet the results our investigation produced were only marginally more indicative of degraded POBM in the peripheral. This suggests that there may be a plateaued or asymptotic relation between POBM and peripheral eccentricity, contrary to the "unscalably poor" response resulting from [11]'s investigation. Though, the slight contradiction in conclusions may be due to the small range tested in [11] (0° - 12°), as opposed to our larger range (0° - 40°).

Finally, though the discoveries act contrary to the concept of survival value and evolutionary applicability, they align with what we know to be true of peripheral vision. It distorts, blurs, and warps the incoming light representing a percept - it is far less effective and retains far less acuity than the foveal region of our FOV. It stands to reason that POBM is hindered in the peripheral region of the human FOV, after having been subject to its many visual transformations prior to cortical reception.

# 7. Conclusions

Given this investigation's results, in tandem with the findings of [11], we can say with little doubt that peripheral eccentricity has a negative effect on a human's capability to perceive biological motion. We have statistically proven that in the peripheral region of the human FOV, one's POBM is severely degraded. Moreover, the human perception of atypical and profile walkers is greatly hampered by dot removal as indicated in even the raw data plots. Both of these conclusions make intuitive sense, are consistent with the literature, and serve to confirm our hypotheses.

We have found that peripheral vision degrades the critical threshold of POBM by a margin of approximately 7 dots. Given the MCT in the foveal view of approximately 4 dots, this is an approximate increase in the threshold of 175%, which begs the question - *what is the applicability of POBM in the peripheral concerning a survival situation*? The visual degradation of our stimuli mimics the occlusion of primary anchor points for POBM in real-world scenarios (due to light behaviour, obstruction, etc.). We can take the typical occlusion of primary joints to be around 50%, for argument's sake. If we struggle to discern a walker's direction before a threshold that represents approximately half of a PLW (our PLW is comprised of 28 dots), it is sensible to assume that in a real-world (sensory-saturated) scenario we may find the application of POBM in the periphery a true challenge.

The shortcomings of peripheral vision are also present in our viewpoint dependency analysis. We observe a clear degradation of POBM due to peripheral eccentricity on all levels. However, most intriguingly, the profile viewpoint seems to suffer a considerable drop-off in perceptibility as we move into the peripheral. This would be an interesting point of investigation moving forward. Aside from this interaction, atypical viewpoints are more difficult to perceive irrespective of peripheral eccentricity, which is consistent with the literature.

# 8. Further Work

## 8.1 Reflections and Improvements

As stated prior, there are small improvements that could be made to further refine the data gathered. Moreover, some quality of life changes would have made the experimentation and trials more bearable for our subjects. As before, we would like to reconsider the 4CFA structure of our experiment. We feel that this may have over-saturated our subjects with choice and as such could overwhelm them into selecting a singular answer as their *don't know* option. As such, a potential improvement to be made here is the addition of a dedicated *don't know* option. This would reduce the number of false positives, and render a more accurate representation of the POBM regarding viewpoints. This option could potentially serve to either reduce the overwhelming success rate for the frontal viewpoint or increase the underwhelming success rate for the profile viewpoint in the peripheral.

Additionally, to further reconcile the differences in recognition of viewpoints, it would help to record false positives. Strictly speaking - should we carry out the experiments again - we would record all user input and classify the false positives as well as the true positives. This would grant us insight into the sensitivity and specificity of the subject's performance in the viewpoint realm. Constructing confusion matrices would also grant insight into the subject tendency for guessing - which may even invalidate the *don't know* option discussed above. Finally, subjects noted that at some points the experiment grew tiresome due to there being no indication of progress. To amend this, we would also recommend the incorporation of a **non-intrusive** progress bar (fairly simple to implement within `PsychToolbox`).

Reflecting upon the project itself, and subject feedback, we are very pleased. We feel that considering the strenuous nature of the stimuli, the tedium of our trials, and the jarring nature of the experiment, most subjects were positive about their experience. Feedback was fairly constructive, and we found that conducting preliminary trials to pilot our experiment was additive to our understanding of the data. It also served to better define any improvements needed to be made. Moreover, we feel we worked extremely effectively as partners and managed a large volume of work and analysis over the duration of the project. Completing the project to this degree has been triumphant for both of us and we have found the process engaging and stimulating.

## 8.2 Future Study and Practicality

We would recommend the continuation of this project with a greater sample space. Moreover, we support studies which seek to further quantify the seeming plateau of POBM falloff in the peripheral. This can be carried out by simply duplicating our (or [11]'s) technique across a far greater range of eccentric increments. It would grant a novel insight into the true relation between peripheral vision and POBM with the foundational understanding of this relationship over both small and large ranges provided by our studies.

We also believe that it is a worthwhile pursuit to investigate the relationship between the perceptibility of the profile viewpoint and peripheral eccentricity. The interaction observed in our data warrants further study in this direction, and we feel as though this could be an intriguing pursuit. This could be achieved simply by wholly registering user input, and analysing subject response specificity, sensitivity and accuracy.

Biological walkers in the periphery are important in many scenarios - including pedestrians or road workers crossing roads relative to drivers. If we acknowledge that we cannot discern the relative direction of a profile walker in our peripheral based on statistical evidence, preventative and protective measures for safety around roads could become more targeted.

Further concerning viewpoint angle research, the literature is rich in azimuth investigation. However, there is very little study conducted concerning the psychometric effects of elevational viewpoint angles. With multi-story smart buildings, and motion-detection security becoming more prevalent, elevational human model recognition is becoming more sought after. Quantifying the human POBM from elevational viewpoints could serve to refine walker intelligibility and recognition in biomimetic computer systems [14].

Finally, we would recommend a machine learning or classification direction. We believe that classification of PLW stimuli could present a unique pathway for POBM research. Though peripheral eccentricity does not necessarily apply to computer vision, viewpoint dependency does. If a computer can achieve a higher degree of accuracy in classification than a human can in their peripheral, this would be a promising start. This sort of study has broad applications in the rapidly growing computer vision industry (in autonomous vehicles for example). A highly accurate human-based model has yet to be developed under the guise of POBM [26] - we feel this could be a novel and interesting direction for further study.

## References


[1] M. H. Johnson, "Biological motion: a perceptual life detector?" *Current Biology*, vol. 16, no. 10, pp. R376–R377, 2006.

[2] P. Murphy, N. Brady, M. Fitzgerald, and N. F. Troje, "No evidence for impaired perception of biological motion in adults with autistic spectrum disorders," *Neuropsychologia*, vol. 47, no. 14, pp. 3225–3235, 2009.

[3] G. Vallortigara, L. Regolin, and F. Marconato, "Visually inexperienced chicks exhibit spontaneous preference for biological motion patterns," *PLoS biology*, vol. 3, no. 7, p. e208, 2005.

[4] E. Grossman, M. Donnelly, R. Price, D. Pickens, V. Morgan, G. Neighbor, and R. Blake, "Brain areas involved in perception of biological motion," *Journal of cognitive neuroscience*, vol. 12, no. 5, pp. 711–720, 2000.

[5] B. I. Bertenthal, D. R. Proffitt, and S. J. Kramer, "Perception of biomechanical motions by infants: implementation of various processing constraints." *Journal of Experimental Psychology: Human Perception and Performance*, vol. 13, no. 4, p. 577, 1987.

[6] G. Johansson, "Visual perception of biological motion and a model for its analysis," *Perception & psychophysics*, vol. 14, no. 2, pp. 201–211, 1973.

[7] A. Jaywant, M. Shiffrar, S. Roy, and A. Cronin-Golomb, "Impaired perception of biological motion in parkinsonâs disease." *Neuropsychology*, vol. 30, no. 6, p. 720, 2016.

[8] T. Mahalingam and M. Subramoniam, "A robust single and multiple moving object detection, tracking and classification," *Applied Computing and Informatics*, 2020.

[9] J. M. Hausdorff, A. Lertratanakul, M. E. Cudkowicz, A. L. Peterson, D. Kaliton, and A. L. Goldberger, "Dynamic markers of altered gait rhythm in amyotrophic lateral sclerosis," *Journal of applied physiology*, 2000.

[10] R. Rosenholtz, "Capabilities and limitations of peripheral vision," *Annual review of vision science*, vol. 2, pp. 437–457, 2016.

[11] H. Ikeda, R. Blake, and K. Watanabe, "Eccentric perception of biological motion is unscalably poor," *Vision research*, vol. 45, no. 15, pp. 1935–1943, 2005.

[12] J. M. Wood, R. A. Tyrrell, R. Marszalek, P. Lacherez, A. Chaparro, and T. W. Britt, "Using biological motion to enhance the conspicuity of roadway workers," *Accident Analysis & Prevention*, vol. 43, no. 3, pp. 1036–1041, 2011.

[13] J. E. Cutting *et al.*, "A program to generate synthetic walkers as dynamic point-light displays," *Behavior Research Methods & Instrumentation*, vol. 10, no. 1, pp. 91–94, 1978.

[14] J. Martinez, R. Hossain, J. Romero, and J. J. Little, "A simple yet effective baseline for 3d human pose estimation," in *Proceedings of the IEEE International Conference on Computer Vision (ICCV)*, Oct 2017.

[15] M. J. Farah, J. W. Tanaka, and H. M. Drain, "What causes the face inversion effect?" *Journal of Experimental Psychology: Human perception and performance*, vol. 21, no. 3, p. 628, 1995.

[16] C. L. Reed, V. E. Stone, S. Bozova, and J. Tanaka, "The body-inversion effect," *Psychological science*, vol. 14, no. 4, pp. 302–308, 2003.

[17] M. Pavlova and A. Sokolov, "Orientation specificity in biological motion perception," *Perception & Psychophysics*, vol. 62, no. 5, pp. 889–899, 2000.

[18] P. Neri, M. C. Morrone, and D. C. Burr, "Seeing biological motion," *Nature*, vol. 395, no. 6705, pp. 894–896, 1998.

[19] J. Beintema, K. Georg, and M. Lappe, "Perception of biological motion from limited-lifetime stimuli," *Perception & Psychophysics*, vol. 68, no. 4, pp. 613–624, 2006.

[20] S. M. Thurman and E. D. Grossman, "Temporal "bubbles" reveal key features for point-light biological motion perception," *Journal of Vision*, vol. 8, no. 3, pp. 28–28, 2008.

[21] V. Ahlström, R. Blake, and U. Ahlström, "Perception of biological motion," *Perception*, vol. 26, no. 12, pp. 1539–1548, 1997.

[22] N. F. Troje, "Decomposing biological motion: A framework for analysis and synthesis of human gait patterns," *Journal of vision*, vol. 2, no. 5, pp. 2–2, 2002.

[23] N. F. Troje and A. Basbaum, "Biological motion perception," *The senses: A comprehensive reference*, vol. 2, pp. 231–238, 2008.

[24] D. Chicco and G. Jurman, "The advantages of the matthews correlation coefficient (mcc) over f1 score and accuracy in binary classification evaluation," *BMC genomics*, vol. 21, no. 1, pp. 1–13, 2020.

[25] K. Zchaluk and D. H. Foster, "Model-free estimation of the psychometric function," *Attention, Perception, & Psychophysics*, vol. 71, no. 6, pp. 1414–1425, 2009.

[26] E. Yurtsever, J. Lambert, A. Carballo, and K. Takeda, "A survey of autonomous driving: Common practices and emerging technologies," *IEEE access*, vol. 8, pp. 58 443–58 469, 2020.

# Appendix A MATLAB® Code

## A.1 Data Processing

weibull_psych_fit.m

```
function crit = psych_fit_weibull(DATA)
% DATA = subject success input (1 = success, 0 = fail)

    % Visual degradation
    NOISE = [2 4 8 12 16 20 24];
    NOISE_ = linspace(0,max(NOISE),1000);

    % Inline functions
    fnBound = @(bhat) 1/(eps+double((bhat(1) > 0) & (bhat(2) > 0)));
    fnPsychometric = @(lam,k,x) 0.25 + 0.75*(1 - exp(-power(max(0,x)/lam
        ,k)));
    fnCost = @(bhat) sum(power(fnPsychometric(bhat(1),bhat(2),NOISE) -
        mean(DATA,1),2)) * fnBound(bhat);

    % Find lowest cost function
    best_fval = 1/eps;
    for iistart = 1:1000
      BHAT0 = [3 1];
      if (iistart > 1)
        BHAT0 = [2+4*rand() 3*rand()];
      end
      [bhat,fval] = fminsearch(fnCost, BHAT0);
      if (fval < best_fval)
        best_fval = fval;
        best_bhat = bhat;
      end
    end

    % Fit psychometric curve
    PM_ = fnPsychometric(bhat(1),bhat(2),NOISE_);

    % Determine threshold, that is, where the fitted function = 0.625
    crit = NOISE_(min(find(PM_ > 0.625)));
end
```

bootstrap_conf_int.m

```
% Load data
load("total_fourty.mat")
load("total_zero.mat")

% Define vars
BOOT = 1000;
DATA = totalZeroArray;

% Bootstrap and store crit
for dat = 1:2
    for NBOOT = 1:BOOT
        for deg = 1:size(DATA,2)
            data = DATA(:, deg);
            ix = ceil(length(data) * rand(length(data),1));
```

```
            data_{dat}(:, deg) = data(ix); % resample _with_ replacement
        end
        crit(NBOOT, dat) = psych_fit_weibull(data_{dat});
    end
    DATA = totalFourtyArray;
end

% Plot data
close all;
figure; hist(crit(:,1)); axis square
title("0^o Eccentricity Critical Threshold Distribution", FontSize=24)
ylabel(sprintf("Number of Bootstrap Results Per Group (out of %.0f)",
    BOOT))
xlabel("Critical Threshold Bootstrap Groups")
figure; hist(crit(:,2)); axis square
title("40^o Eccentricity Critical Threshold Distribution", FontSize=24)
ylabel(sprintf("Number of Bootstrap Results Per Group (out of %.0f)",
    BOOT))
xlabel("Critical Threshold Bootstrap Groups")
```

## A.2 Data Collection and Stimuli Construction

biowalker_trials.m

```
    %% PSYCH SETUP
% Clear the workspace and the screensca

sca;
close all;
clearvars;

% Here we call some default settings for setting up Psychtoolbox
PsychDefaultSetup(2);

% Set window to opacity for debugging
PsychDebugWindowConfiguration(0, 1);

% Get the screen numbers
screens = Screen('Screens');
screenNumber = max(screens);

% Open an on screen window
[window, windowRect] = PsychImaging('OpenWindow', screenNumber, [200 200
    200]);

% Get the size of the on screen window
[screenXpixels, screenYpixels] = Screen('WindowSize', window);

% Query the frame duration
ifi = Screen('GetFlipInterval', window);

%% TRIAL MATRIX SETUP
num_trials = 4;
theta_v = [90, 120, 150, 180];
degradation = [2,4,8,12,16,20,24];
eccentricity = [0, 40];

trial_rand = {};

```

```
35 for i = 1:num_trials
36     trial_rand = [trial_rand, randomiseTrials(theta_v, degradation,
           eccentricity)];
37 end
38
39 %% DOT SETUP2
40 % Colour intensity
41 colourLevel = 1;
42
43 % We can define a center for the dot coordinates to be relaitive to.
       Here
44 % we set the centre to be the centre of the screen
45 trueDotCenter = [(screenXpixels / 2) (screenYpixels / 2)];
46 dotCenter = [(screenXpixels / 2 - 140) (screenYpixels / 2 + 500)];
47
48 dotYpos = 0;
49 dotXpos = 0;
50 dotSizes = 10;
51
52 white = WhiteIndex(screenNumber);
53 dotColours = white*colourLevel;
54
55 % Sync us and get a time stamp
56 Screen('Flip', window);
57 waitframes = 1;
58
59 % Maximum priority level
60 topPriorityLevel = MaxPriority(window);
61 Priority(topPriorityLevel);
62
63 % Draw White Dot on screen
64 Screen('DrawDots', window, [dotXpos; dotYpos], dotSizes, dotColours,
       trueDotCenter, 2);
65 Screen('Flip', window);
66
67 time = 0;
68 data_count = 1;
69 life_count = 0;
70
71 len = 1000;
72 scale = 2;
73
74 inputKey = cell(1,size(theta_v,2)*size(degradation,2));
75
76 for trial = 1:size(trial_rand, 2)
77     % Flash grey
78     Screen('TextFont', window, 'Arial Unicode MS');
79     Screen('TextSize', window, 125);
80     DrawFormattedText(window, num2str(trial_rand{trial}.eccentricity), '
           Center', 'Center', [0, 0, 0]);
81     Screen('Flip', window);
82
83     KbStrokeWait;
84
85     % Reset black
86     Screen('FillRect', window, [0, 0, 0]);
87
88     Screen('Flip', window);
89
90     trajData = getTrajData(trial_rand{trial}.degradation, trial_rand{
```

```
        trial}.theta_v, 'TrajectoryData/*.mat', scale);
91      while (~validKey(trial_rand{trial}.inputKey))
92          [~, ~, keyCode, ~] = KbCheck;
93          trial_rand{trial}.inputKey = KbName(keyCode);
94
95          if (mod(life_count, len/50) == 0)
96              trajData = getTrajData(trial_rand{trial}.degradation,
                    trial_rand{trial}.theta_v, 'TrajectoryData/*.mat', scale)
                    ;
97          end
98
99          % Extract dotXpos and dotYpos and apply to dot on screen
100         if time <= 1
101             for i = 1:length(trajData)
102                 dotXpos = trajData{2, i}.array(1, data_count)/scale;
103                 dotYpos = -trajData{2, i}.array(3, data_count)/scale;
104                 Screen('DrawDots', window, [dotXpos; dotYpos], dotSizes,
                        white, dotCenter, 2);
105             end
106         else
107             Screen('FillRect', window, [0.5, 0, 0]);
108         end
109
110         % Flip to the screen
111         Screen('Flip', window);
112
113         % Increment the time
114         time = time + ifi;
115
116         data_count = incrementValues(data_count, time) + 1;
117         life_count = incrementValues(life_count, time);
118
119     end
120     Screen('FillRect', window, [100, 100, 100]);
121     Screen('Flip', window);
122
123     data_count = 1;
124     pause(0.5);
125
126     trial_rand = populateCorrect(trial_rand, trial, trial_rand{trial}.
            inputKey);
127     time = 0;
128 end
129
130 % Clear screen
131 sca;
132
133 matrix = dataParser(trial_rand, theta_v, degradation, eccentricity);
134
135 % Keep useful vars
136 clearvars -except matrix num_trials;
137
138 name = input("Trial Subject Name: ", "s");
139 cd TrialData/Store/
140 save(sprintf("%s-%s.mat", date, name))
141 cd ../..
```

rotate_axis.m

```
function traj3Drot = rotateAxis(traj3D, theta, vp)
    if (vp == "overhead")
        % Rotation Matrix for overhead rotation
        A = [1 0 0; 0 cosd(theta) -sind(theta); 0 sind(theta) cosd(theta
            )];
        traj3Drot = A*traj3D;
    elseif (vp == "profile")
        % Rotation Matrix for profile rotation
        A = [cosd(theta) sind(theta) 0; -sind(theta) cosd(theta) 0; 0 0
            1];
        traj3Drot = A*traj3D;
    end
end
```

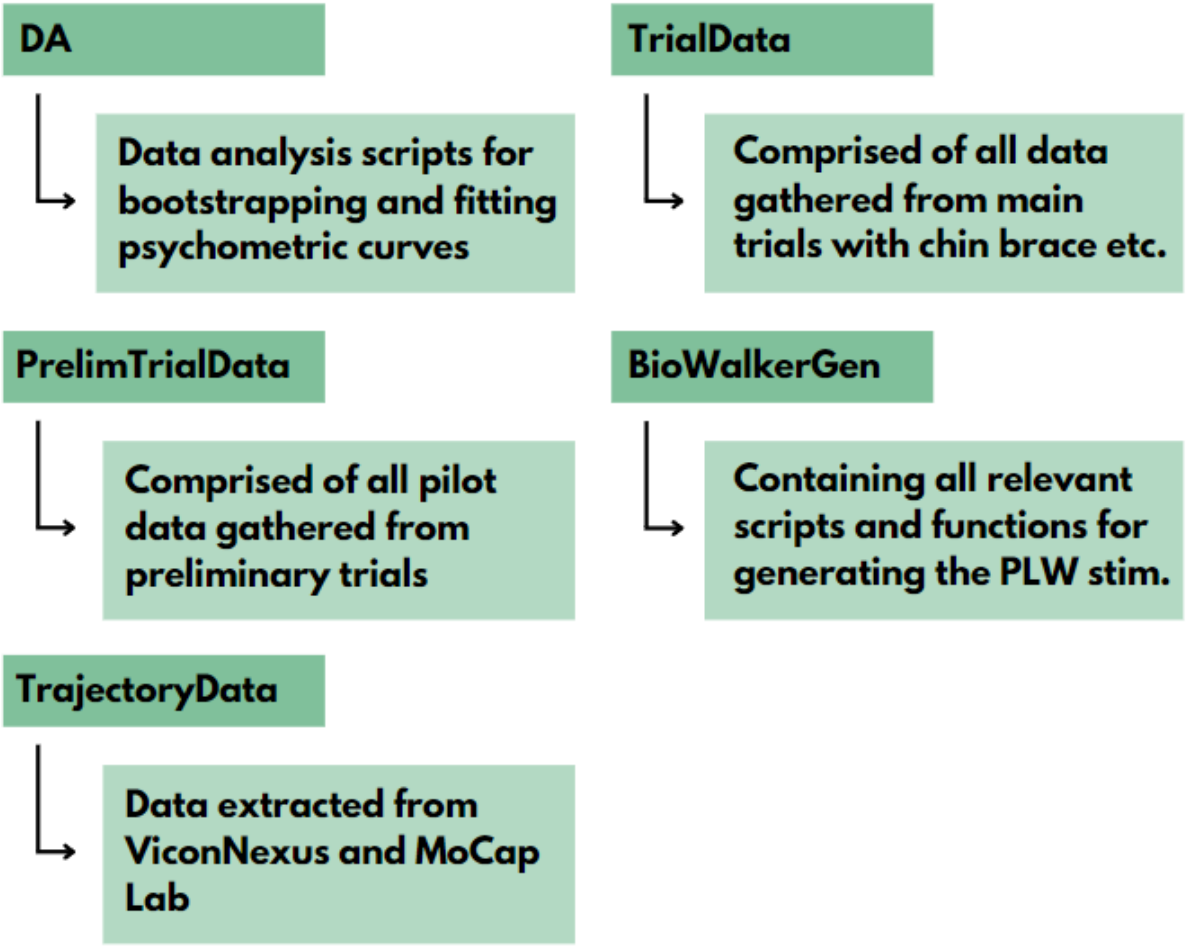


**Figure A15** Graphical representation of directory management for our experiment.

# Appendix B Relevant Data

## B.1 Viewpoint Graphs

### *B.1.1 Psychometric Curves*

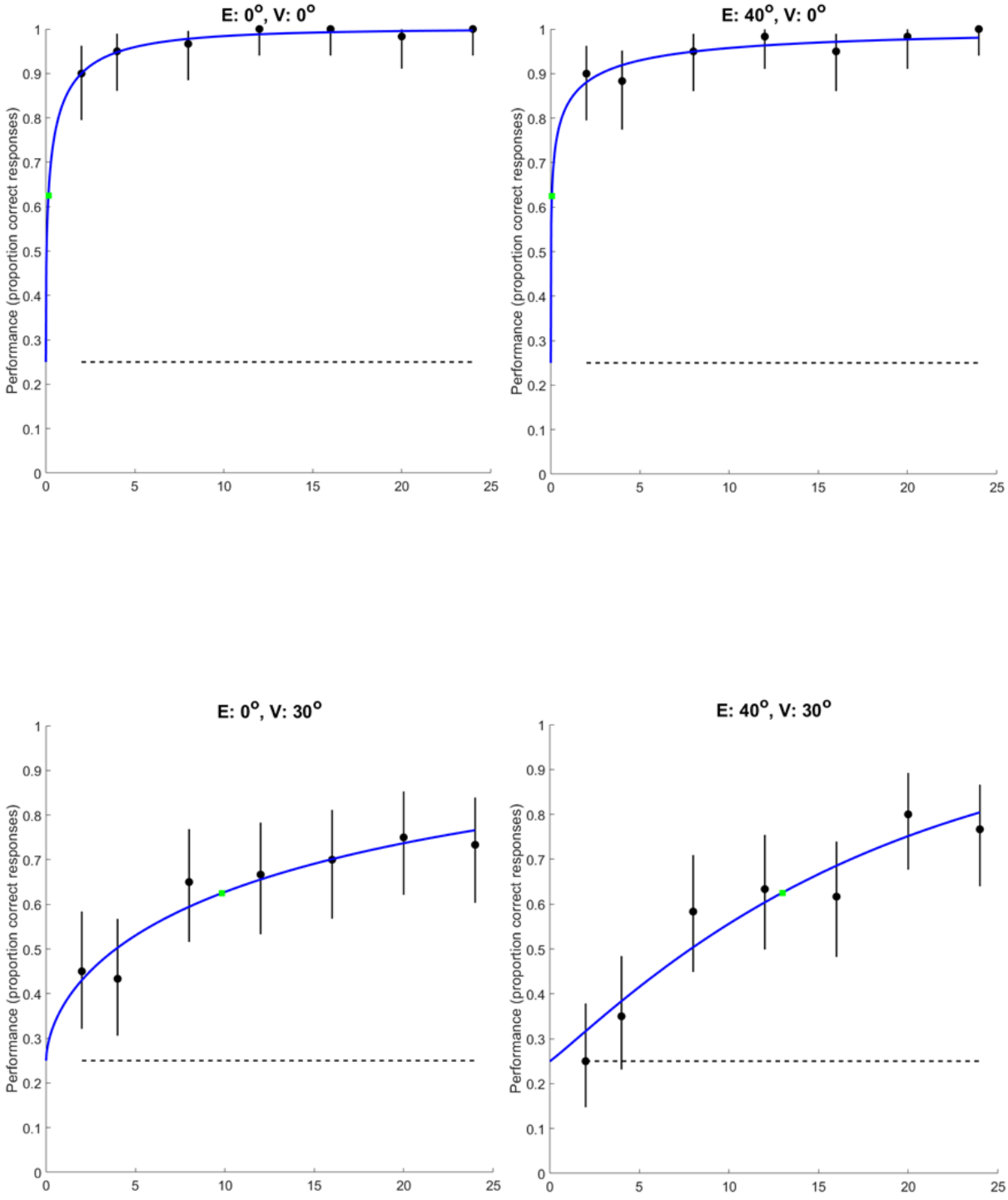

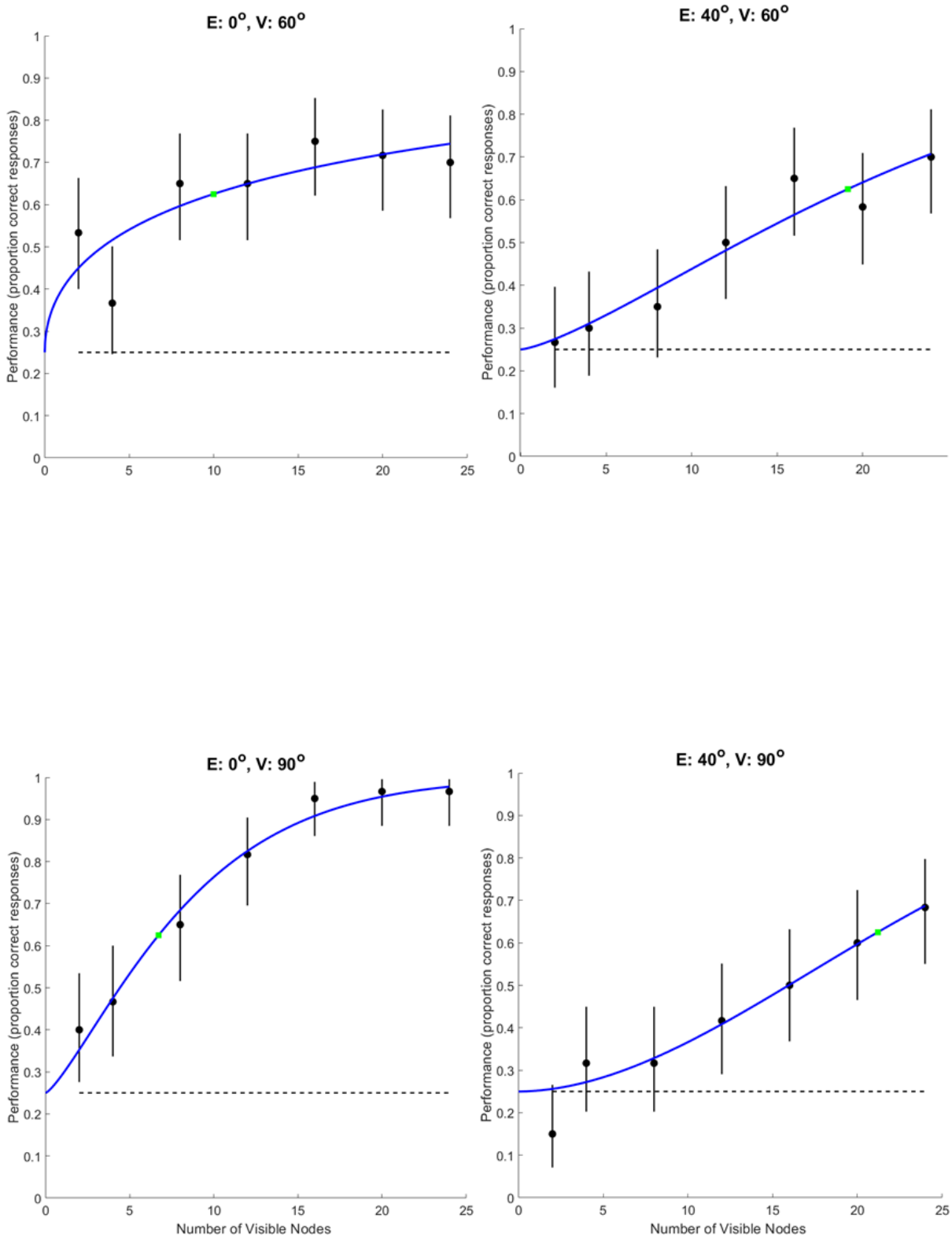


**Figure B16** Psychometric curves fitted to raw viewpoint data.

### *B.1.2 Bootstrap Histograms*

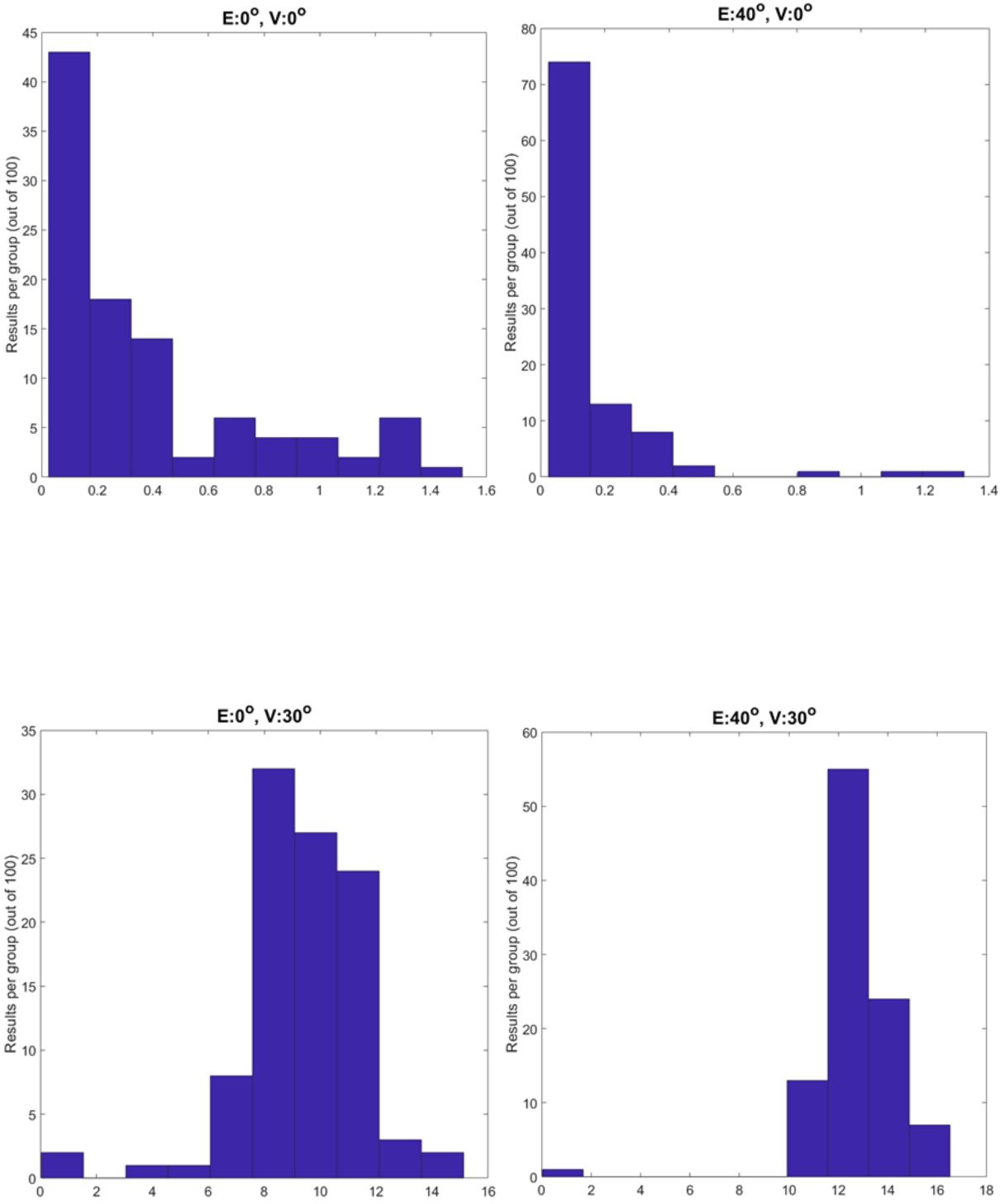

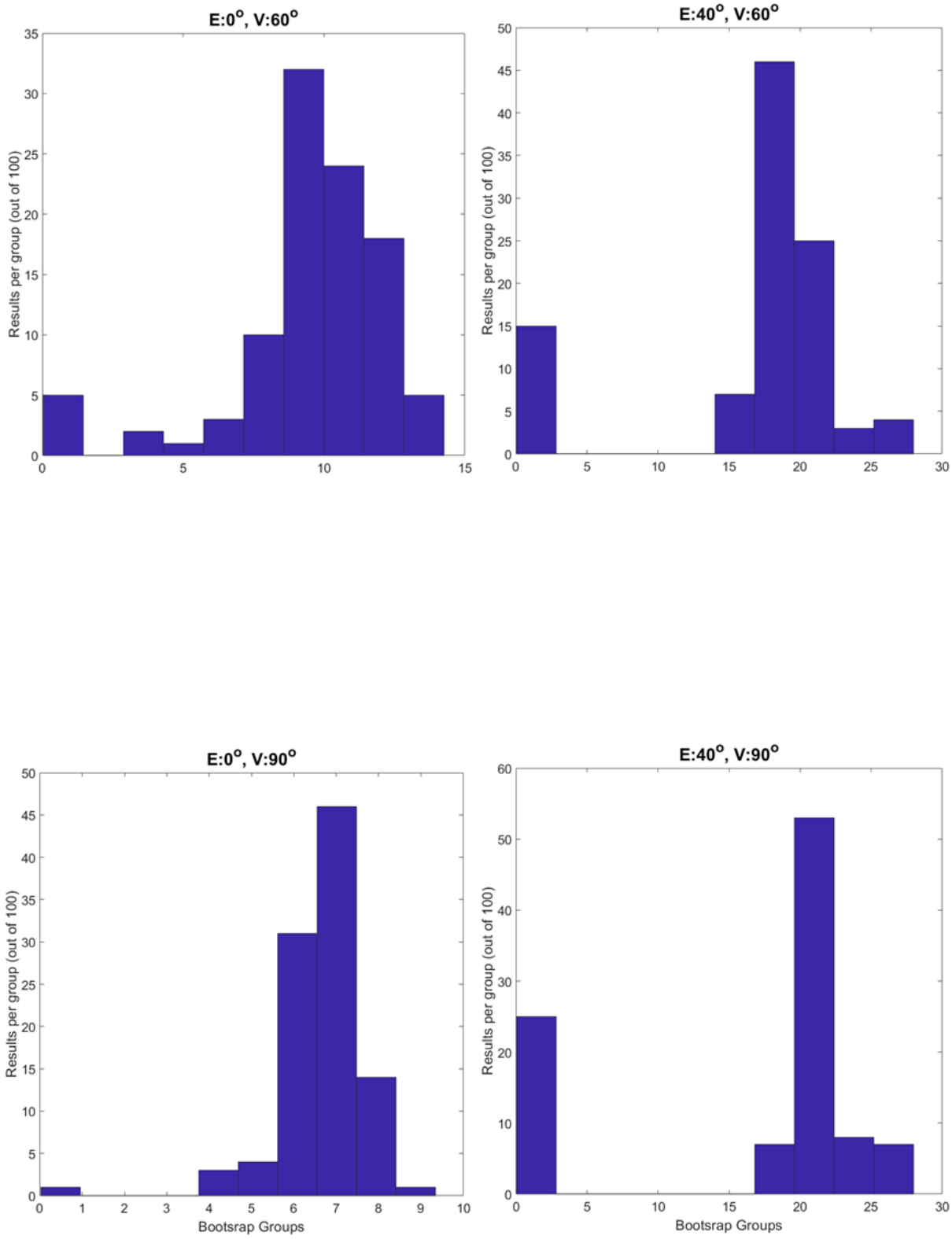


**Figure B17** Bootstrapped histograms for psychometric viewpoint data.